#25-045
2025 AFS Proceedings ©American Foundry Society

Optimizing 3D Printable Filaments for Printed Expendable Patterns in Lost Foam Casting

Jacob A Belke
Sean M Frank
Mercury Marine, Fond du Lac, Wisconsin, USA

ABSTRACT

The lost foam casting process offers significant advantages, including the elimination of parting lines and cores, leading to reduced machining and material waste. However, the traditional method of creating foam patterns involves expensive and time-consuming tooling, which limits the process's flexibility and cost-effectiveness, particularly for low-volume production and rapid prototyping. 3D printing emerges as a transformative solution to these challenges, allowing for the direct fabrication of complex lost foam patterns without the need for traditional tooling. Despite these advancements, a significant knowledge gap remains in the selection of appropriate materials for 3D printed patterns. Sixteen 3D printable materials were assessed for use as expendable printed patterns using thermogravimetric analysis (TGA) and casting trials. Variants of polyethylene performed the best in TGA and casting trials, but face printing challenges. High impact polystyrene (HIPS) was designated the best overall and shown to be improved further with plasticizers and foaming agents.

Keywords: aluminum, lost foam, additive manufacturing, 3D printing, polymer, thermogravimetric analysis, TGA

INTRODUCTION

Lost foam casting is a metalcasting process that has gained significant traction in various industries due to its ability to produce complex geometries with high precision and minimal waste. The process consists of a molded foam pattern, typically from expanded polystyrene (EPS), coated with a permeable refractory material that is embedded in sand before molten metal is poured into the mold, causing the foam to vaporize, and be replaced by the metal. One of the primary advantages of lost foam casting is its ability to produce highly intricate and precise castings with minimal need for cores or parting lines, which are typically required in traditional sand casting. However, parting lines or glue lines may still be present if the foam patterns are assembled. The flexibility of the process allows for the casting of complex geometries that would be difficult or impossible to achieve with other casting methods.

Despite the benefits, one of the significant challenges associated with lost foam casting is the production of the foam patterns themselves. Traditionally, these patterns are manufactured using complex molding and assembly tools, which can be expensive and time-consuming to produce. Tools can range from $10,000 for a 20 x 20 inch to $100,000 for a 40 x 40 inch (depending on complexity) and take up to 18 weeks to complete. The cost of tooling is particularly high for low-volume production runs, where the initial investment may not be justified. Additionally, the lead time required to produce the tooling can be a significant bottleneck, particularly in industries where time-to-market is critical. This is further exacerbated by the fact that any design changes typically require modifications to the tooling, resulting in additional costs and delays. Consequently, the traditional approach to producing foam patterns can be a limiting factor in the widespread adoption of lost foam casting for certain applications, especially in situations where rapid prototyping or design iteration is necessary.

The utilization of 3D printing technology offers a unique solution to the challenges posed by traditional foam pattern production in lost foam casting. Miller and Iverson validated the use of 3D printed molding tools, but the cost to print tools has been found to be unjustifiable compared to traditional subtractive machining methods.[1] The 3D printing process allows for the direct fabrication of lost foam patterns from digital models, eliminating the need for costly and time-consuming tooling.[2] This technology significantly reduces lead times, enabling rapid prototyping and facilitating iterative design processes. Despite the promising advantages of 3D printing in lost foam casting, there remains a significant knowledge gap regarding the optimal materials for 3D printed patterns.[3]

3D printing lost foam patterns is a relatively new application, so the material properties required for successful casting, such as thermal stability, vaporization characteristics, and compatibility with various metals, are not yet fully understood. Expanded polystyrene has well-documented properties and performance metrics and alternative pattern materials to EPS have been shown to be viable. Guler et al. experimented with expanded polyethylene (EPE) as an aluminum lost foam pattern material and found some success under the right

conditions.[4] Belke et al. used a bio-derived polylactic acid (PLA) bead for pattern material with success in aluminum and cast iron.[5] 3D printing introduces a variety of new materials, each with different behaviors during the casting process. Foreseeable challenges include 3D printing materials may not vaporize as cleanly as conventional foams potentially leading to defects in the final casting, unfavorable interactions between the printed pattern material and the refractory coating, as well as its behavior under the high temperatures of molten metal. Handayani et al. evaluated three different printed materials for their castability but did not identify the underlying material property for their success.[3] Addressing the material selection knowledge gap is crucial for optimizing the process and ensuring that 3D printed patterns can consistently produce high-quality castings. This paper aims to investigate the castability of various 3D printable materials to determine the polymer properties that influence the success of printed expendable patterns.

MATERIALS AND METHODS

The 3D printable materials tested consisted of 15 different readily available fused filament fabrication (FFF) materials and one stereolithography (SLA) wax resin with an EPS control (Table 1).

Table 1. Materials Trialed Along With Filament Brand

Brand	Materials
Matterhackers	Acrylonitrile Butadiene Styrene (ABS), Polylactic acid (PLA), Polyvinyl Acetate (PVA), Nylon with carbon fibers (NX), High Impact Polystyrene (HIPS)
Colorfabb	Lightweight Polylactic acid (LW-PLA)
Filaments.ca	High Density Polyethylene (HDPE), Linear Low-Density Polyethylene (LLDPE)
Polymaker	Polyvinyl Butyral (PVB), Polycarbonate (PC)
I-Beam	Polylactic acid + wax (PLA+W)
Moldlay	Wax-like plastic (WAX)
BuMat	Polypropylene (PP)
Aibecy	Polycaprolactone (PCL)
3DXTECH	Polycarbonate + Acrylate-Styrene-Acrylonitrile (PC/ASA)
Formlabs	SLA castable wax resin

TENSILE BAR PRINTING

A hollow tensile bar (Figure 1) was chosen for the test piece to compare the castability of the multiple filaments. Twelve tensile bars of each FFF material were printed using a Raise3D N2 Plus fully enclosed dual extruder 3D printer. Six resin tensile bars were printed on a Formlabs Form 2 SLA 3D printer giving a total of 186 tensile bars.

Parts were printed with a 0.6 mm brass nozzle, except for the nylon with carbon fibers (NX) which used a hardened steel nozzle, at 0.2 mm layer height, one wall, and no infill. Print temperatures, speeds, fan speeds, and flow rates were optimized for each material, per brand recommendations, and printer to ensure the best print quality, with specific settings adjusted as needed for lightweight polylactic acid (LW-PLA) and other materials, ensuring that the tensile bar (Figure 1) was accurately printed.

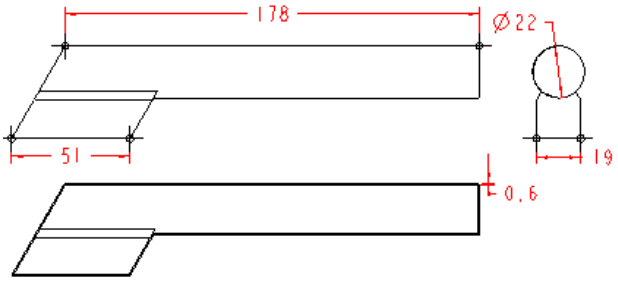

Figure 1. A schematic drawing of the hollow tensile bar used in the casting trial. Dimensions shown in red (mm).

CASTING

Printed tensile bars (Figure 2) were glued at the top and bottom of an EPS sprue (1.6 pcf) (Figure 3) with 3M hot melt adhesive 3762. The gating consisted solely of the 51 x 19 mm bottom surface indicated in Figure 1. Tensile bar sprue clusters were dip coated using ASK Ceramcote FS-502 with a permeability range of 100-120. Patterns were dried at 115 ±5F (46 ±3C) for 24 hours before casting. Pattern clusters were compacted in 40 GFN synthetic mullite sand heated to 130F (54C) and poured with A356 at 1450 ±15F (787 ±8C) using a robotic ladling system (Figure 4). Molds were cooled for an hour before the castings were extracted and degated. Castings were shotblasted before being X-rayed for porosity/inclusions and measured using digital calipers.

Figure 2. Examples of printed tensile bars (Figure 1) in five different materials.

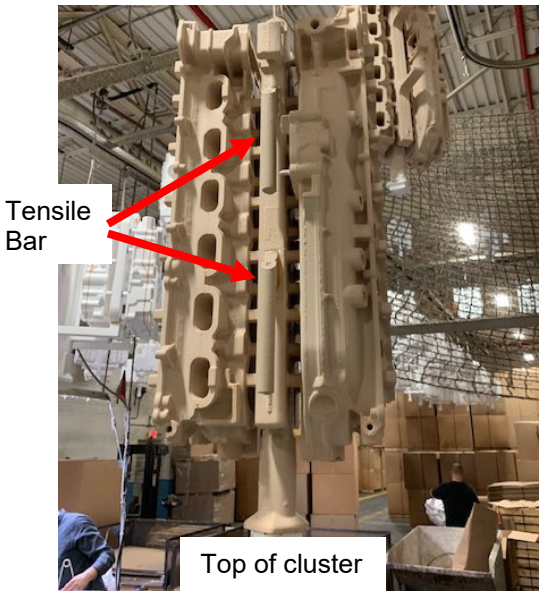

Figure 3. Printed and coated tensile bars glued to the top and bottom of a sprue. Tensile bars are bottom filled.

Figure 4. Robotic pouring system at Mercury Marine, Fond du Lac, Wisconsin. (Image courtesy of Mercury Marine.)

RESULTS

THERMOGRAVIMETRIC ANALYSIS (TGA)

Thermogravimetric decomposition data for EPS and 16 3D print materials is shown in Table 2. Bieniewicz et al. showed that materials that decompose at or lower temperatures than EPS perform well for lost foam.[6] Eight materials decompose at a lower temperature than EPS, but of those only two (PLA+W and WAX) fully decomposed.

Table 2. TGA Results for 15 Different 3D Print Materials and the EPS Control (Red). Materials are Ranked in Order of Ascending Decomposition Time

Material	Onset Temp. (C)	End Temp. (C)	Time to Decompose (Sec)	Temp. at 0 Mass (C)	% Residue
HDPE	477	508	94	659	0.06
LLDPE	459	497	112	651	0.10
LW-PLA	353	392	115	-	0.83
NX	455	493	115	-	6.59
EPS	**406**	**450**	**130**	**642**	**0.31**
PP	440	485	133	-	6.20
HIPS	427	475	139	663	0.10
PLA+W	353	402	145	662	0.16
PC	507	557	147	-	25.40
PLA	348	399	150	-	5.02
WAX	350	403	159	647	0.34
ABS	422	479	168	-	1.45
PC/ASA	409	467	172	-	13.25
PVB	372	432	178	-	2.39
PCL	361	428	199	-	7.76
Castable Wax (SLA)	397	474	233	-	0.95
PVA	287	401	344	-	6.84

TENSILE BAR CASTING LENGTH

Tensile bar lengths measured after casting were compared to the as-printed lengths (Figure 5). Linear Low-Density Polyethylene (LLDPE) closely resembled EPS in TGA and performed the best of the filaments tested. The polyvinyl acetate (PVA) tensile bars warped in the drying oven due to the hygroscopic properties of PVA during dipping that expanded at elevated temperatures causing the prints to elongate beyond the original dimensions. The time to decompose was weakly related to the cast lengths (Figure 6) with a faster decomposition time tending to result in a longer cast bar. Cast bars were X-rayed showing porosity in the top portion of the bars (Figure 7).

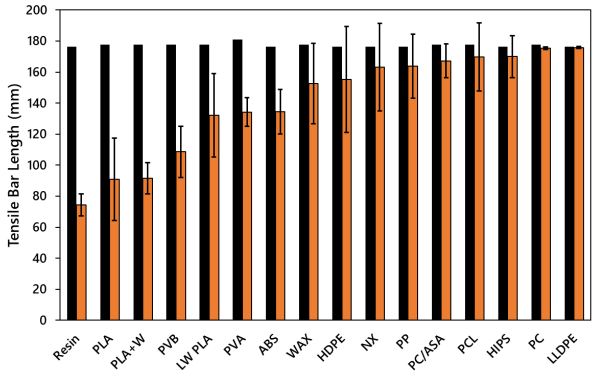

Figure 5. Average tensile bar length after printing (black) and after casting (orange). Error bars are 95% standard deviation of the mean. Error bars for the printed length are less than 0.2 mm and not displayed.

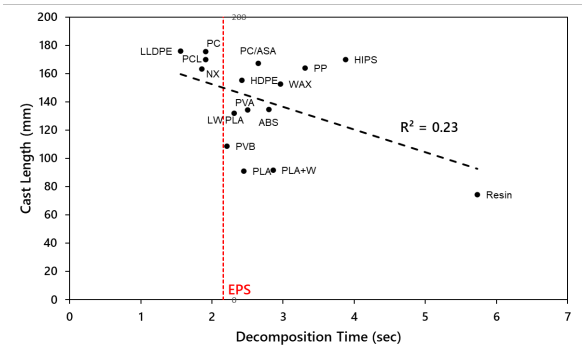

Figure 6. Cast length related to the decomposition time for all tested materials. Cast lengths generally increased inverse of the decomposition time. EPS decomposition time represented by red dashed line.

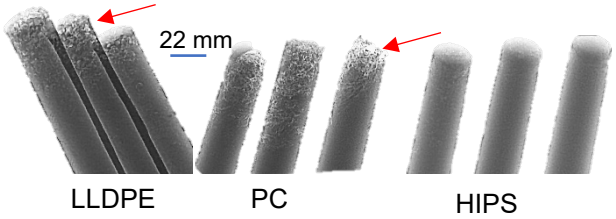

Figure 7. X-ray images of three cast tensile bars from the three best performing printed materials based on cast length. Red arrows annotate porosity in the castings which appear as lighter areas.

DISCUSSION

POLYMER DECOMPOSITION CHARACTERIZATION

In the characterization of polymer decomposition, understanding the relationship between polymer structure and thermal behavior is crucial. The decomposition characteristics of polymers are influenced by their molecular structure, chemical composition, and specific intermolecular interactions. Linear polymers with simple, high-density structures decompose quickly at higher temperatures, while those with more complex compositions or significant hydrogen bonding decompose at lower temperatures and take longer. Branched and networked polymers generally show intermediate behavior, with their properties influenced by the presence of rubbery phases or cross-linking.

Relationship between Structure and Decomposition Characteristics

Polymers exhibit distinct structural configurations (Figure 8) that significantly influence their thermal and mechanical properties (Table 3, Figure 9). Linear polymers feature long, unbranched chains, which can range from simple to complex depending on the degree of crystallinity and chain alignment. Branched polymers have chains that branch out from a central backbone. This branching creates a less dense molecular structure compared to linear polymers, affecting their crystallinity and thus their thermal properties. The moderate chain entanglement leads to decent thermal stability but with slightly reduced strength compared to linear polymers. Networked polymers are characterized by a three-dimensional network of interconnected chains, often cross-linked to form a stable matrix. This network structure imparts rigidity and dimensional stability, but the extensive cross-linking can also make the material more prone to incomplete decomposition and higher residue. Blended polymers or copolymers combine two or more distinct polymer types to achieve balanced properties. These blends can exhibit intermediate properties that reflect the characteristics of the constituent polymers, often resulting in improved overall performance by leveraging the strengths of each component while mitigating their individual weaknesses. Each structural configuration imparts unique properties to the polymers, making them suitable for various applications based on their thermal stability, mechanical strength, and processing characteristics.

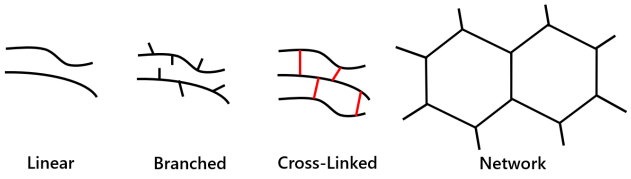

Figure 8. Illustration of the four types of polymer structures.

Polyethylene (PE) Variants

The high density polyethylene (HDPE) and LLDPE exhibit relatively high onset temperatures of decomposition, with HDPE starting at 891F (477C) and LLDPE at 858F (459C). HDPE, with its linear structure and high degree of crystallinity, demonstrates a robust thermal stability and a higher temperature at complete decomposition. The high degree of chain entanglement in HDPE contributes to its thermal stability, as the entangled polymer chains create a strong network that resists decomposition. In contrast, LLDPE, which has a more

branched structure compared to HDPE, shows a somewhat lower decomposition onset and end temperatures. The reduced chain entanglement in LLDPE leads to a less rigid structure, making it less thermally stable than HDPE, resulting in a lower temperature at zero mass and somewhat faster decomposition.

Table 3. Summary of Onset Temperatures for Various Polymers Grouped by Structure Type

Structure	Polymers (Onset Temp. (C))	Average Onset Temp. (C)
Linear with short branches	LLDPE (459)	459
Linear with some degree of branching	PP (440)	440
Linear with a rubbery phase	HIPS (427)	427
Linear with grafted rubbery phases	ABS (422)	422
Linear blend	PC/ASA (409)	409
Networked	EPS (406)	406
Linear	HDPE (477), Nylon (455), PC (507), PLA (348), PVB (372), PCL (361), PVA (287)	401±80

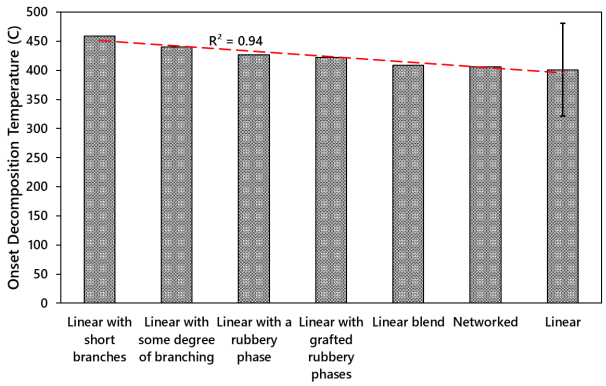

Figure 9. Average decomposition start temperature by polymer structure from Table 2 and Table 3. Error bars are 95% standard deviation of the mean.

Polylactic Acid (PLA) Variants

The PLA and PLA+W exhibit lower onset decomposition temperatures, with PLA starting at 658F (348C) and PLA+W at 667F (353C). The PLA+W demonstrates a higher end decomposition temperature compared to pure PLA, indicating that the wax additive stabilizes the polymer at elevated temperatures. The lower thermal stability of PLA can be attributed to its ester bonds, which are more susceptible to hydrolysis at elevated temperatures compared to the more robust carbon-carbon bonds in other polymers. The relatively lower chain entanglement in PLA contributes to its lower onset temperature and relatively fast decomposition. PLA+W shows improved thermal stability, which can be partially attributed to better entanglement or interaction between PLA and the additive, enhancing its resistance to decomposition.

Polypropylene (PP) and Polystyrene (HIPS)

The PP decomposes between 824F (440C) and 905F (485C) with a time to decompose of 133 seconds, showing good thermal stability but leaves a residue compared to HDPE. The PP has a somewhat crystalline structure with moderate chain entanglement. Its thermal stability is reflected in its decomposition onset temperature. High impact polystyrene (HIPS), which contains a synthetic rubber additive (polybutadiene), starts decomposition at 801F (427C) and completes it at 887F (475C). The incorporation of the polybutadiene creates additional chain entanglements and interactions within the polymer matrix, contributing to higher onset temperature than EPS while decomposing to completion.

Engineering Polymers

The polycarbonate (PC) shows the highest onset temperature at 945F (507C), and an end temperature of 1035F (557C) where the residue remained stable up to the 1292F (700C) test temperature. This high thermal stability is due to the strong carbonate bonds present in PC, which resist breakdown at high temperatures. The high chain entanglement in PC further contributes to its robust thermal stability. In contrast, polycarbonate + acrylate-styrene-acrylonitrile (PC/ASA) decompose between 768F (409C) and 873F (467C) with a residue left, indicating that the blend has a lower thermal stability over unmodified polycarbonate. The PC/ASA blend benefits from a certain degree of chain entanglement, although not to the extent of pure PC.

Other Polymers

The PVA has a much lower onset temperature of 549F (287C) and a significantly longer decomposition time of 344 seconds, which is attributed to its high polarity and extensive hydrogen bonding that reduces thermal stability and slows the decomposition process. Castable wax (SLA) begins decomposing at 747F (397C), close to that of EPS, but it takes considerably longer to decompose, with a time of 233 seconds, due to its large molecular wax structure. The polycaprolactone (PCL), with an onset temperature of 682F (361C) and a decomposition time of 199 seconds, exhibits intermediate thermal stability. While it decomposes at a lower temperature than EPS, its greater chain entanglement slows down the decomposition process, resulting in a longer time to decompose compared to EPS.

CASTING

The lost foam casting process, like other casting processes, is an energy balance problem.[6] A successful casting only occurs if the energy cost of expending the foam pattern, energy loss to the mold, and other thermal losses (radiation) are lower than the superheat thermal energy of the metal so that solidification occurs after filling is complete. Energy loss to the sand and other thermal losses are negligible if the casting process parameters are in control like sand temp, metal temp, etc. leaving the energy contained in the pattern the controlling variable. The EPS pattern energy is typically controlled through monitoring the mass density (ρ) during foam pattern molding. The traditional pattern density range used for EPS patterns cannot be applied to other printed materials as there is a difference in material energy density (U). This in-part explains the differences in cast lengths (Figure 5) along with the structural dependencies discussed previously.

Lower mass density materials are not always the answer as aerogels, for example, are the lowest density engineering materials (~1 $\frac{kg}{m^3}$ (0.06 $\frac{lb}{ft^3}$)) but have a melting point of 2192F (1200C) meaning aluminum cannot expend it. The energy density of a pattern can be determined by calculating the energy required to vaporize the material starting from room temperature. Suitable pattern materials can be selected based on their individual energy requirements compared to EPS which is known to work.

EPS

The energy requirements for expending the EPS tensile bar (Figure 1) can be calculated using Equations 1 & 2 where Q is the total heat transfer, mass (m), temperature (T), and enthalpy (H). Equations 1 & 2 are used to calculate the heating curves representing the relationships between phase-transition temperatures (Figure 10) using data from Table 4. The EPS tensile bar has a volume of 90.18 cm^3 (5.50 in^3) and assuming a foam pattern density of 25.63 $\frac{kg}{m^3}$ (1.60 $\frac{lb}{ft^3}$), the tensile bar weights 2.31 grams. The energy required to heat and vaporize the EPS tensile bar is 3.82 kJ giving an energy density of 42.4$\frac{J}{cm^3}$. Expending the EPS tensile bar using A356 would result in a temperature drop of 31.9°F (17.7°C) (Equation 1).

$$Q_{heat} = m * C_p * \Delta T \qquad \text{Eqn. 1}$$

$$Q_{phase\ change} = m * \Delta H_{phase\ change} \qquad \text{Eqn. 2}$$

Table 4. Thermodynamic properties of EPS used for calculating energy density. (Inverse of the enthalpy of polymerization was used for ΔH_{DP})

Heat Capacity ($C_{p,solid}$)	1.45 $\frac{J}{g\,℃}$ [7]
Melting Temperature (T_M)	250C [5]
Enthalpy of Fusion (ΔH_M)	4.61 $\frac{J}{g}$ [5]
Heat Capacity ($C_{p,liquid}$)	2.25 $\frac{J}{g\,℃}$ [8]
Depolymerizing Temperature (T_{DP})	391C [5]
Enthalpy of Depolymerization (ΔH_{DP})	645 $\frac{J}{g}$ [9]
Enthalpy of Vaporization, Styrene ($\Delta H_{V,C_8H_8}$)	363 $\frac{J}{g}$ [9]

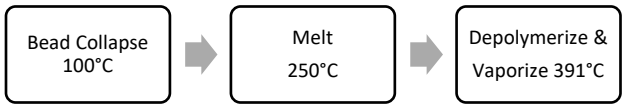

Figure 10. EPS pattern expending process during filling.

1. Heating solid EPS from room temperature to melting
$$Q = 2.31g * 1.45\frac{J}{g\,℃} * (250 - 25)C = 754J$$
2. Melting EPS
$$Q_M = 4.61\frac{J}{g} * 2.31g = 11J$$
3. Heating liquid EPS from melting temperature to depolymerization temperature
$$Q = 2.31g * 2.25\frac{J}{g\,℃} * (391 - 250)C = 731J$$
4. Depolymerizing EPS to styrene
$$Q_{DP} = 645\frac{J}{g} * 2.31g = 1490J$$
5. Vaporizing styrene
$$Q_{V,C_8H_8} = 363\frac{J}{g} * 2.31g = 839J$$
$$Total = 3825\,J$$
$$U = \frac{3825\,J}{90.18\,cm^3} = 42.4\frac{J}{cm^3}$$

PLA

The PLA had one of the worst casting performances, only second to the resin print. PLA started to decompose at a lower temperature than EPS but took 20 seconds longer and did not completely decompose leaving 5% residue (Table 2). The energy requirements to expend the printed PLA tensile bar (Figure 11) with a 0.6 mm wall thickness can also be calculated using Equations 1 & 2 along with the data from Table 5. The PLA tensile bar has a printed wall volume of 9.67 cm^3 (0.59 in^3). This differs from the EPS pattern as all the mass of the printed tensile bar is concentrated at the printed walls versus the EPS being evenly distributed throughout the volume. Assuming a

solid printed wall density of 1240 $\frac{kg}{m^3}$ (77.4 $\frac{lb}{ft^3}$), the tensile bar weights 12 grams.

The energy required to heat and vaporize the PLA tensile bar is 19.23 kJ giving an energy density of 1988 $\frac{J}{cm^3}$ which is five times more energy to expend and 47 times denser (U) than EPS. For comparison, if the same printed volume is used for EPS, in the case of HIPS, the energy requirement to expend is 16.65 kJ (13% less than PLA). Expending the PLA tensile bar using A356 would result in a temperature drop of 160.6°F (89.2°C) (Equation 1). The higher energy density of PLA is hypothesized to contribute to its poor casting performance.

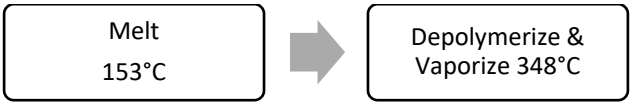

Figure 11. PLA pattern expending process during filling.

Table 5. Thermodynamic properties of PLA used for calculating energy density. The inverse of the enthalpy of polymerization was used for ΔH_{DP}. $\Delta H_{V,C_6H_8O_4}$ was estimated using Joback method

Heat Capacity ($C_{p,solid}$)	1.31 $\frac{J}{g\,℃}$ [10]
Melting Temperature (T_M)	153C [11]
Enthalpy of Fusion (ΔH_M)	91 $\frac{J}{g}$ [10]
Heat Capacity ($C_{p,liquid}$)	1.66 $\frac{J}{g\,℃}$ [10]
Depolymerizing Temperature (T_{DP})	348C
Enthalpy of Depolymerization (ΔH_{DP})	374 $\frac{J}{g}$ [12]
Enthalpy of Vaporization, Lactide ($\Delta H_{V,C_6H_8O_4}$)	646 $\frac{J}{g}$ (Joback)

LLDPE

The LLDPE was the best performing printed polymer in the casting trials. LLDPE started to decompose (Figure 12) at a higher temperature than EPS but decomposed faster and completed at a very similar temperature to EPS (Table 2). The energy density theory, however, contests the viability of LLDPE as the energy required to heat and vaporize the LLDPE tensile bar is 48.86 kJ giving an energy density of 5053 $\frac{J}{cm^3}$ which is 13 times more energy to expend and 119 times denser (U) than EPS. The high energy level is a product of LLDPE's high ΔH_{DP} (Table 6).

Depolymerization of polypropylene and polyethylene is very energy intensive requiring very high temperatures due to the polymer being a lean vinyl polymer with few substitute monomers and a high electronic stabilization by the side chains.[13] This makes it likely that LLDPE, HPDE, and PP did not depolymerize but rather vaporized as a whole polymer or the high temperatures resulted in other side reactions. If the depolymerization step is subtracted from the energy summation, the energy requirement to expend the LLDPE drops to 14.21 kJ or four times greater than EPS but 15% lower than HIPS.

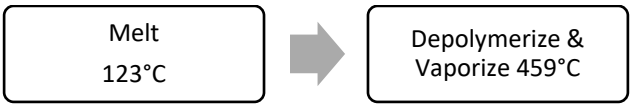

Figure 12. The LLDPE pattern expending process during filling.

Table 6. Thermodynamic Properties of LLDPE Used for Calculating Energy Density

Heat Capacity ($C_{p,solid}$)	2.34 $\frac{J}{g\,℃}$ [14]
Melting Temperature (T_M)	123C [15]
Enthalpy of Fusion (ΔH_M)	86 $\frac{J}{g}$ [15]
Heat Capacity ($C_{p,liquid}$)	2.57 $\frac{J}{g\,℃}$ [16]
Depolymerizing Temperature (T_{DP})	459C
Enthalpy of Depolymerization (ΔH_{DP})	3863 $\frac{J}{g}$ [17]
Enthalpy of Vaporization, Ethylene ($\Delta H_{V,C_2H_4}$)	483 $\frac{J}{g}$ [18]

OPTIMIZING PRINTED PATTERN

Select 3D printed filaments have been shown to be successful alternatives to EPS patterns but still lack some desirable attributes for lost foam casting. The LLDPE has a fast decomposition time (Table 2) and performed the best in the casting trial (Figure 5) although having a high amount of gas porosity (Figure 7). Unfortunately, the material is extremely challenging to printing due to its high thermal expansion causing issues like warping and delamination, failing the manufacturing criteria. The PC also performed well in the casting trial (Figure 5) again with a high amount of gas porosity (Figure 7) likely caused by the incomplete decomposition of the filament (Table 2). Additionally, PC has similar printing challenges as LLDPE but of lesser magnitude making it printable, but not desirable. The HIPS decomposition curve is nearly identical to EPS (Table 2), has good cast length average (Figure 5), no gas porosity (Figure 7), and is easily printable making it the material of choice based on the materials tested.

The HIPS/PS material properties can be modified to improve castability through the addition of plasticizers. Bieniewicz et al. showed the time for an aluminum metal front to pyrolyze a PS based glue joint decreased with increasing amounts of wax and other plasticizers.[6,19] Plasticizers increase in distance between polymer chains, improving their mobility and help reduce entanglement

which can decrease the enthalpy and temperature of phase transformations.

The easiest improvement independent of material is the reduction of mass. Decreasing the wall thickness of the tensile bar from 0.6 mm to 0.4 mm reduces the energy requirements by 30%. This reduces the temperature loss of A356 using HIPS from 139°F (77.2°C) to 95.9°F (53.3°C) respectively. Reducing the wall thickness of a part can have some undesirable effects such as incomplete printed walls and wall collapse during sand compaction. Alternatively, printed mass can be reduced using foaming agents mixed into the polymer that expands during printing. The LW-PLA is a modified PLA containing a foaming agent and showed a 45% longer cast length over standard PLA (Figure 5). Ali et al. used LW-PLA with different sand mold types and was successful in producing castings from the material.[20] Additional lightweight versions of printing materials are starting to emerge with applications to 3D printed lost foam patterns.[21]

CONCLUSION

Sixteen 3D printable materials were assessed for use as expendable printed patterns using thermogravimetric analysis (TGA) and casting trials. The analysis of polymer decomposition behaviors reveals that molecular structure, chemical composition, and chain entanglement are critical factors influencing thermal stability and decomposition characteristics. Linear polymers, such as HDPE and PC, exhibit higher onset temperatures and faster decomposition times due to strong intermolecular forces and robust chain networks, while more branched or networked polymers like PP and ABS show moderate thermal stability. Variants of polyethylene performed the best in TGA and casting trials, but face printing and gas porosity challenges. High impact polystyrene (HIPS) was designated the best overall with EPS like decomposition characteristics, high cast length, low porosity with potential to be improved further with plasticizers and foaming agents.

ACKNOWLEDGMENTS

This research was funded by Brunswick Corporation.

REFERENCES

1. Miller, M., Iverson, G., “The Viability of 3D Printed Lost Foam Molds,” Paper #24-11 presented at: AFS Metalcasting Congress, 2024; Milwaukee, WI (2024).
2. DeBruin, M., Jordan, S.E., Inventors, “Process for Evaporative Casting,” US 2024/0017320 A1.(January 18, 2024).
3. Handayani, Wagner, N., Okhuysen, V., Seitz, M., Garibaldi, K., “Utilization of 3D Printed Materials in Expendable Pattern Casting Process,” Paper presented at: 2020 *Light Metals* (2020).
4. Guler, K.A., Karaaslan, A., Kisasöz, A., “A study of expanded polyethylene (EPE) pattern application in aluminium lost foam casting,” *Russian Journal of Non-Ferrous Metals*, 56(2):171-176 (April 2015).
5. Belke, J., Kopper, A., Sheets, T., Mueller, D., Bhargava, S., Mercy, C., “Bio-based Foam Patterns for Lost Foam Casting,” *AFS Transactions* (2025).
6. Bieniewicz, K., Reich, M., Soraruf, N., Steer, A., Sanders, P., Belke, J., “Improving Metal Flow in Lost Foam Casting Through Use of Low Thermal Degradation Hot Melt Adhesives,” *International Journal of Metalcasting* (April 2024).
7. Khoukhi, M., Abdelbaqi, S., Hassan, A., Darsaleh, A., “Impact of dynamic thermal conductivity change of EPS insulation on temperature variation through a wall assembly,” *Case Studies in Thermal Engineering,* 25:100917 (March 2021).
8. Judovits, L.H., Bopp, R.C., Gaur, U., Wunderlich, B., “The heat capacity of solid and liquid polystyrene, p-substituted polystyrenes, and crosslinked polystyrenes,” *Journal of polymer science, Part B, Polymer physics*, 24(12):2725-2741 (Dec. 1986).
9. National Oceanic and Atmospheric Administration, “Styrene Monomer, Stabilized,” Cameo Chemicals, (June 1999). Chrome-extension://efaidnbmnnnibpcajpcglclefindmkaj/https://cameochemicals.noaa.gov/chris/STY.pdf. (Link last accessed 01-30-25.)
10. Pyda, M., Bopp, R.C., Wunderlich, B., “Heat capacity of poly(lactic acid),” *The Journal of Chemical Thermodynamics*, 36(9):731-742 (Sept 2004).
11. Kaczmarek, H., Nowicki, M., Vuković-Kwiatkowska, I., Nowakowska, S., “Crosslinked blends of poly(lactic acid) and polyacrylates: AFM, DSC and XRD studies,” *Journal of Polymer Research*, 20 (March 2013).
12. Masutani, K, Kimura, Y., “PLA Synthesis, From the Monomer to the Polymer,” In: Jiménez, A., Peltzer, M., Ruseckaite, R., eds. Poly(lactic acid) Science and Technology: Processing, Properties, Additives and Applications: The Royal Society of Chemistry (2014).
13. Diaz-Silvarrey, L.S., Zhang, K., Phan, A.N., “Monomer recovery through advanced pyrolysis of

waste high density polyethylene (HDPE)," *Green Chemistry*, 20:1813-1823 (March 2018).
14. Sobolciak, P., Karkri, M., Al-Maadeed, M.A., Krupa, I., "Thermal characterization of phase change materials based on linear low-density polyethylene, paraffin wax and expanded graphite," *Renewable Energy*, 88:372-382 (April 2016).
15. Coben, C., Sancaktar, E., "Use of Pyrolyzed Soybean Hulls as Fillers in Polypropylene and Linear Low Density Polyethylene," *Sustainable Chemistry*, November 2021;2(4):622-644.
16. Thomas, L.C., "Characterization Of Melting Phenomena In Linear Low Density Polyethylene By Modulated Dsc," TA Instruments, TA-227.
17. Roberts, D.E., "Heats of Polymerization, A Summary of Published Values and Their Relation to Structure," *Journal of Research of the National Bureau of Standards*, March 1950;44:221-232.
18. National Oceanic and Atmospheric Administration. "Ethylene," Cameo Chemicals. June 1999. chrome-extension://efaidnbmnnnibpcajpcglclefindmkaj/https://cameochemicals.noaa.gov/chris/ETL.pdf. (Accessed August 2024.)
19. Pederson, T.C., Inventor, "Glued lost foam casting pattern assembly," US 7,318,468 B2. (November 16, 2008).
20. Ali, M.A., Huseynov, O., Fidan, I., Vondra, F. "Lost-PLA Casting Process Development Using Material Extrusion with Low-Weight PLA," Paper presented at: *34th Annual International Solid Freeform Fabrication Symposium*, 2023; Austin, Texas.
21. Belke, J.A., Inventor, "3-D printable expendable lost foam pattern," US 12012495 B1 (June 18, 2024).